CosmicWatch

An Attempt at Building a Muon Detector

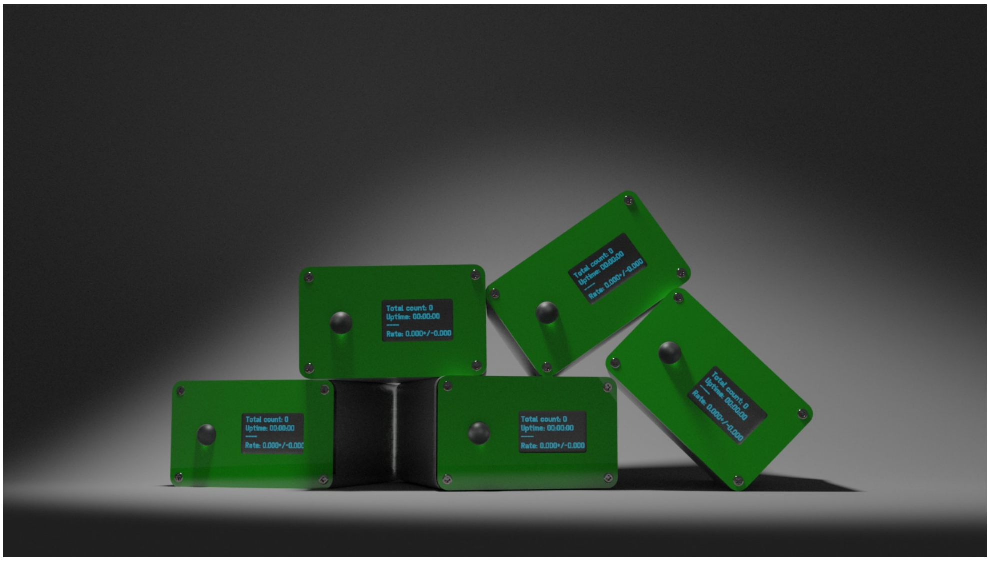

Coolen Finn	-	i6223502
Gévers Nicolas	-	i6256388
Hangelbroek Renée	-	i6257707
Louveau Nicolas	-	i6247013
Palmerio Jeremy	-	i6239656
Ranaudo Guglielmo	-	i6244080
Roussel Edgar	-	i6247698
Verloo Matijs	-	i6255137

Supervisor: Chad Ellington

Maastricht Science Programme
Maastricht University

28 June 2022

Contents

1 Introduction

In the years 1911 and 1912, the physicist Victor Hees made multiple ascents in a hydrogen balloon, in an attempt to make measurements of the radiation in the atmosphere. At a height of 5300 meters he discovered that the rate of ionization was three times more than that at sea level. This lead to the conclusion that the measured radiation had to penetrate the atmosphere from above. From one of his ascent that took place during a partial solar eclipse, he could conclude that this radiation was not caused by the sun since there was no significant drop in the measurements. Thus, the radiation had to come from somewhere else: Cosmic Rays [1].

Around a hundred years later, in 2017, Spencer Axani, Katarzyna Frankiewicz and Janet Conrad in collaboration with Paweł Przewłocki created the CosmicWatch project. A simple, small and portable detector that can measure this radiation, called muons. Even at sea level, since the device amplifies the measured signals [2].

With the help of the data provided by the CosmicWatch project and the previous project group that did an attempted on building one, the initial plan for this project was to build the CosmicWatch and to take measurements around Maastricht. However, due to insufficient supplies and delayed delivery times, this was not possible. So instead, this paper provides as a sort of manual for future groups who attempt on building the muon detector.

2 Theoretical background

Cosmic rays are a form of radiation consisting of high-energy protons and parts of nuclei moving through space at almost the speed of light. They can be emitted by the Sun, known as solar winds, or from inside our galaxy. However, most of their origins are still unknown. Some, not yet conclusive, data from the Pierre Auger Observatory [3] points out that certain originate from starbursts galaxies, galaxies that form very fast, or supernova explosions. Both of which expulse protons and nuclei at high velocities through electromagnetic interactions, but nothing has been consistently proven yet. Cosmic rays are called "primary cosmic rays" when they are still outside the Earth's atmosphere, which deflects most of them. However, a fraction of them produces showers of secondary particles, themselves called "secondary cosmic rays", by tearing apart atoms in violent collisions. In a sort of snowball reaction, these secondary particles keep decaying into other particles until they reach a stable state and/or interact with another particle. Though around 1000 particles hit 1 meter squared of Earth's surface every second, it does not affect us in any dangerous way, as these particles do not interact with our bodies in any harmful way. During the collision of primary cosmic rays with the atmosphere, typical particles produced are mesons, such as positively or negatively charged pions or kaons. These mesons usually decay into muons within a relatively short distance due to their short lifetimes, following this equation:

$$\pi^{\pm} \to \mu^{\pm} + \nu_{\mu}(\nu_{\mu}) \text{ ... } (99{,}98\%)$$
$$K^{\pm} \to \mu^{\pm} + \nu_{\mu}(\nu_{\mu}) \text{ ... } (63{,}5\%).$$

With the percentages at the end of the equations representing the reaction's branching fraction, i.e. the fraction of particle that decay by a specific decay mode, like radioactive decay, with respect to the total number of particles that decay during that reaction.

Muons are unstable particles, classified as leptons like the electron, but with a lifetime of $2.2 * 10^{-6}$ seconds, much shorter than electrons. When muons result from the decay of charged mesons, they usually continue in the same direction as the original cosmic ray with speed close to the speed of light. Without considering relativistic effects, muons could only travel half a kilometer with their speed and lifetime, but Special Relativity describes an effect called length contraction at very high velocities. Muons having a substantially high speed, the distances in its rest-frame are much shorter than the Earth's rest frame, which allows them to survive the flight to the Earth's surface. Though muons have a shorter lifetime than electrons, they have a mass of $1.8 * 10^{-28}$ kg, which is a bit more than 206 times the electron's mass. If a muon and an electron were created simultaneously with the same force by a cosmic ray, the muon being heavier would have less acceleration. In this situation, one would usually think that the muon would travel less distance than the electron because of its lower acceleration. That is where Bremsstrahlung radiation comes in: it is a type of radiation emitted by charged particles when they decelerate, which therefore depends on the particle's acceleration. With a lower acceleration, muons will thus lose less energy through Bremsstrahlung radiation than electrons in an identical interaction. Hence, being heavier allows for this muon flux to penetrate deeper in the Earth's atmosphere and attain depths only a few other particles can.

When pions decay into muons, they can be either become positively charged or negatively charged. As seen in the following equation [4]:

$$\pi^0 \to \gamma \ ,$$
$$\pi^+ \to \mu^+ + \nu_\mu \ ,$$
$$\pi^- \to \mu^- + \bar{\nu}_\mu \ .$$

The muon's charge greatly influences the path that the muon will take due to the Earth's magnetic field. The positively charged muons will be deflected East while the negatively charged muons will be deflected in the West direction. Therefore, positively charged muons are called "westerly" muons and negatively charged ones "easterly" muons. This is called the East-West Effect[4].
Since positively charged muons are 15 to 20% [5] more present than negatively charged muons, there is a significantly larger amount of westerly muons than easterly muons, which causes an asymmetry called the East-West Cosmic Muon Asymmetry Effect. Because majority of particles are westerly muons, it is expected that there is a more substantial muon flux from the west, also shown in collected data[6].
Besides the East-West Cosmic Muon Asymmetry Effect is there also the Latitude Effect which influences the muon's flux. This effect is also caused by Earth's magnetic field and is due to its low deflecting strength near the poles and its high deflecting strength close to the equator. Hence, the Latitude Effect results in a lower muon flux near the equator than near the poles.[7, 8] For later experiments with the muon detector, it will not be possible to measure this effect since all measurements will be made in Maastricht.

3 Methods

3.1 Description of The Circuit

3.1.1 The SiPM

The muon detector is centered around a silicone photomultiplier, often called SiPM, which is a single-photon-sensitive device [9]. When coupled with a plastic scintillator, the SiPM can detect photons created by a muon interacting with the scintillator and translates into a voltage of the order of a couple milivolts, over a fraction of a microsecond. However, the pulses created by the SiPM are too weak and short lived for common microcontrollers to pick up and record, thus the main electronic circuitry in the detector is there to amplify and extend the voltage peaks for an arduino to register. See Figure 1 for the circuit.

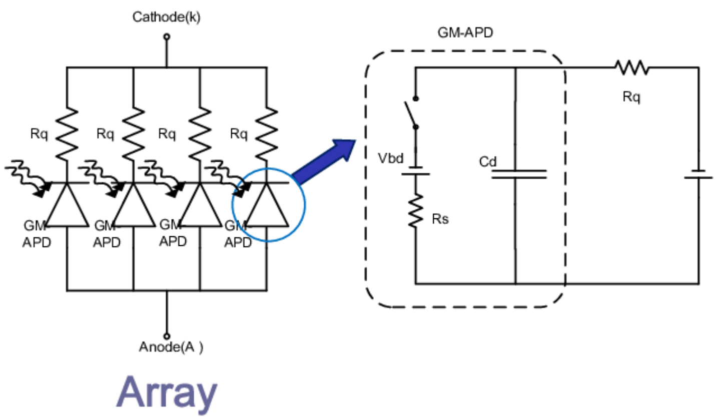

Figure 1: Diagram of a Silicone Photomultiplier. It consists of an array of photosentive diodes which create a small voltage gain between the cathode and anode when a excited by a photon.

3.1.2 Materials

All the materials used in this project were from the list of components provided by the creator of this project Spencer Axani. All links and resources of the original project, as well as the instruction guide, reference list and all the code to upload are available on the creator's Github:

`https://github.com/spenceraxani/CosmicWatch-Desktop-Muon-Detector-v2`

3.1.3 The Circuits

To power the photomultiplier, the 4.6V DC supply to the arduino is boosted to 29.5V thanks to a LT3461 DC-DC booster located on the main PCB. In the SiPM, there are several resistors and capacitors acting as low pass filters to filter out the higher frequency from the photomultiplier. The SiPM PCB is plugged in the main PCB to connect it to power and also to transfer the small voltage spike to the main circuit. This signal is then amplified by a factor of about 24 by a feedback loop through an LT1807 operational amplifier which is then sent to the peak detector circuit [10]. The purpose of this circuit is to extend the pulse, of the order of half a microsecond to an approximately half millisecond pulse which can be recorded by the Arduino Nano. The pulse is extended by combining high valued resistors (R6+R7=200kOhm) and low valued capacitors (C6 = 10nF) to create a decay time of (R6+R7)*C6 =0.5ms. See the entire circuit on Figure 2.

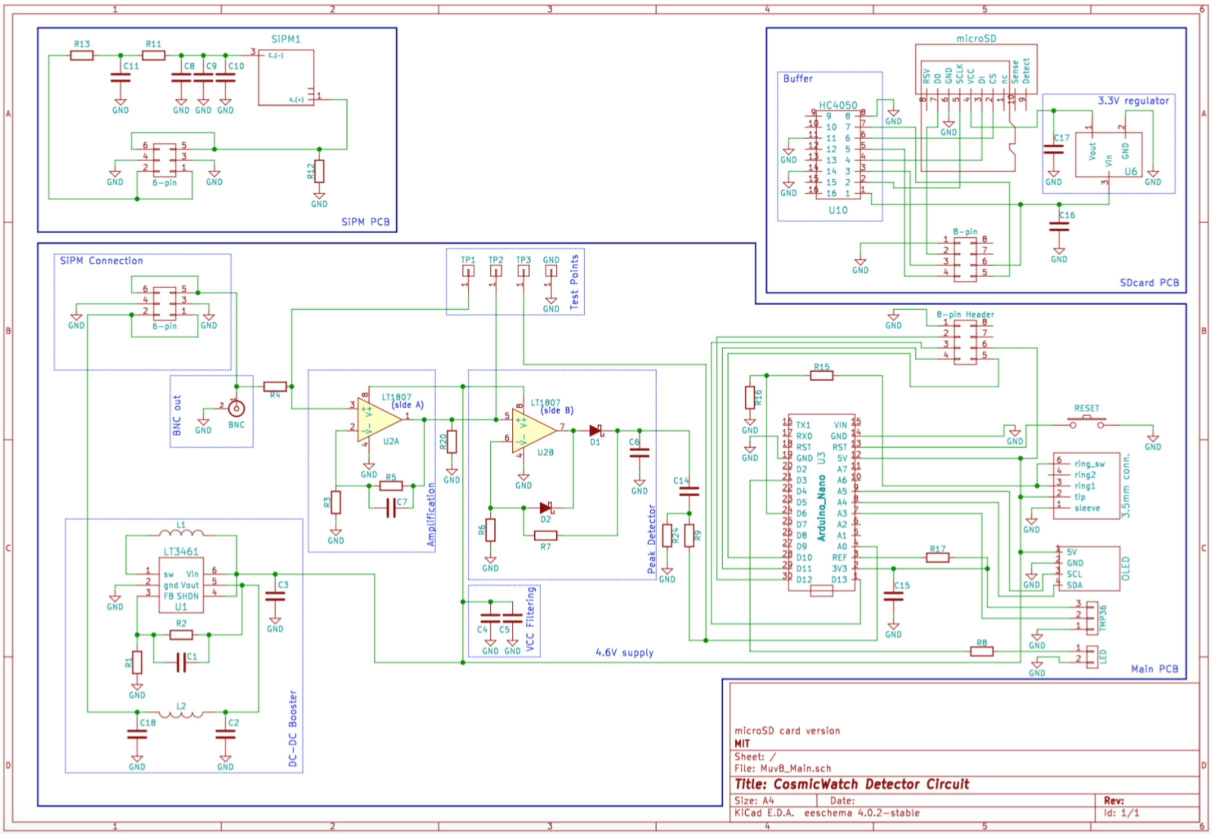

Figure 2: Diagram of the entire muon detector circuit. The dark blue boxes delimit between different PCBs and the thinner blue boxes separate the different circuits.

3.1.4 The Microcontroller

Once the pulse is amplified and extended, it can be registered by the arduino with a theoretical 16MHz clock. In practice though, the arduino takes 90 cycles to to make a measurement which means the sample resolution is brought down to 178kHz [11]. The arduino also allows for programming of the data collected and can be used to process the signal by creating a trigger threshold and calculating the rate in real time. The detectors dead time can also be accounted for by the arduino and some code. This data can then be sent to an OLED screen which is also controlled by the arduino or directly to a computer through the microUSB cable. The data can otherwise by stored on a SD chip for later use. Additional programming can be sent to the arduino to set up multiple detectors in 'coincidence mode'. In this setting, a pair of muon detectors can operate together to distinguish between muon detection which trigger both simultaneously and other background radiation.

3.2 Soldering

3.2.1 The Different Soldering Methods

Soldering consists of connecting two components (in this case, an electrical component to a PCB board) by melting a third material (called the solder) to join them together. In electronics, the solder used is an alloy consisting mainly of lead and tin [12]. To perform electronics soldering, two methods are available:

The first one is using an air gun with some soldering paste. The soldering paste consists of a paste containing some micro-particle of metal. When some heat is applied on it, these particles melt and agglomerate between the component and the PCB board to join them together (see Figure 3).

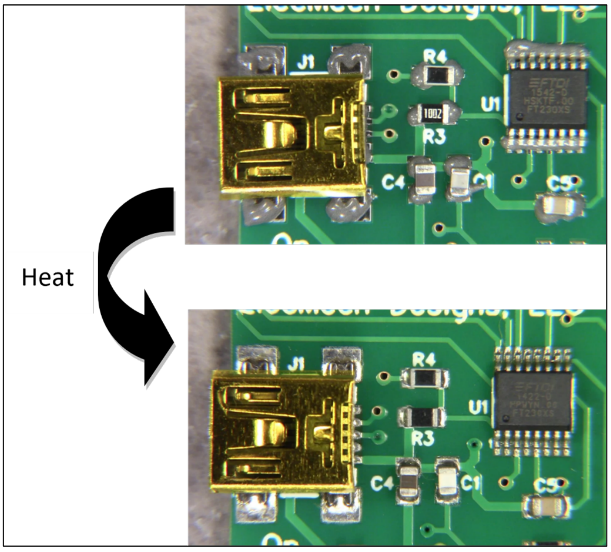

Figure 3: Example of soldering using the soldering paste
[13]

The second method consists of using a hot metallic tip to melt a small amount of solder between the board and the electrical components (Figure 4). For this method, the solder is present in a form of a thin wire (Figure 4 and 5).

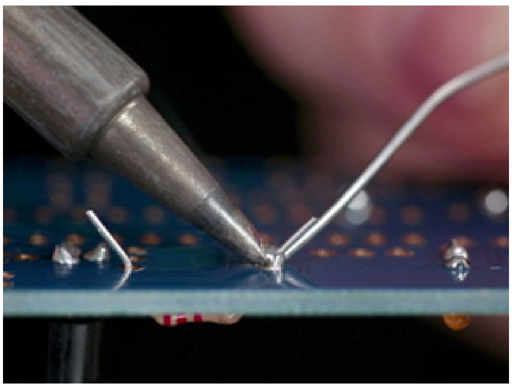

Figure 4: Soldering using a hot tip [14]

Figure 5: A coil of soldering metal [15]

3.2.2 Using The Soldering Station

In this project, the soldering station used is a RS PRO (model number: 124-4134). This station has both an air gun (on the left in Figure 6) and a soldering tip (on the right) with a maximum working temperature of 480 °C and a minimum of 200°C. [16]

Figure 6: Overview of the soldering station [16]

The temperature used in this project to solder electronics components was usually around 300°C or a little bit more (for the soldering tip). This temperature is enough to melt the metal which consists of an alloy of lead and tin. For the air gun, the temperature was set between 300-400 °C. In that range, the temperature is enough to melt the solder in the paste. However if the temperature is too high, it might burn or melt some other part (especially the plastic one). The choice between using either the air gun or the hot tip depends on the situation: Overall, it was noticed that the air gun is more precise and better for small components. Nevertheless, in some situations, using the soldering tip was a better choice; particularly when the air gun would be too close to some other component and melt them (these components being mostly some connector and header that have some plastic part).

3.2.3 Desoldering Components

Since many components were missing during this project period, it was essential to desolder some of the previous group's project to reuse them. To do so, the main tool used was a desoldering pump (see Figure 7). The purpose of this tool is to suck the melted solder to remove it from the board. To melt the solder, the air gun was used most of the time. Unlike the soldering tip, the air gun can heat up a small area of the board which allows to melt multiple contact points at the same time. Indeed, when using the tip, only one or maximum two contact points can be melted simultaneously. Therefore, the air gun had to be used for desoldering the components that have a lot of contact points (such as the op-amp, DC/DC booster, . . .). It is also important to mention that it seems that the temperature to desolder should be a little bit higher than to solder (around 50°C higher).

Figure 7: Desoldering pump

3.3 Ordering The Missing Components

Because lots of components were missing at the beginning of this project; it was necessary to order the missing ones. The usual website used for this project is Digikey (`https://www.digikey.nl/`). However, some complications were faced since it was almost impossible to get the components in time by ordering on this website. Thus an alternative website was used: `https://nl.farnell.com/` . The issues with this website is that not all the components were available (the main one being the op-amp and the DC/DC booster), leading to the necessity to re-use the one of the previous project period by de-soldering them. Proceeding like this might probably damage the components and lead to re-using some components that do not work properly. Most particularly for the op-amp and the DC/DC booster which are some sensitive components.

3.4 Testing

Starting material included a set of four piles of three PCB boards, each representing one unassembled detector, consisting of the main PCB, SiPM PCB and an SD card PCB. Separate from the components mounted onto the PCB boards, bags of previously delivered components which were still in their packaging, ordered by the last project group, were present.

Testing of these boards and components was done in order to determine the condition of starting materials. This would allow ordering of any missing / dysfunctional components and assessing the possibility of reusing the last project group's PCB boards. Before anything else, the piles of PCBs were mixed and matched to see if any combination of boards formed a functioning muon detector when assembled. No combination resulted in a functional detector, confirming the need for testing.

3.4.1 Instrumentation

The VOLTCRAFT SMD-200 multimeter (see Figure 8) is a multimeter created appropriately for testing and measuring surface mounted components. These proved to be useful for the simpler components, however, later testing required more specialised instrumentation. Some of the resistors and capacitors had such small values that these multimeters could not register them.

The RIGOL DS1052D Oscilloscope (see Figure 9) was required for measuring and visualising the signal at the test points during the later mentioned guided troubleshooting process. The first oscilloscope used was not working correctly, hindering said troubleshooting process and overall project progress.

Figure 8: The SMD multimeter [17]

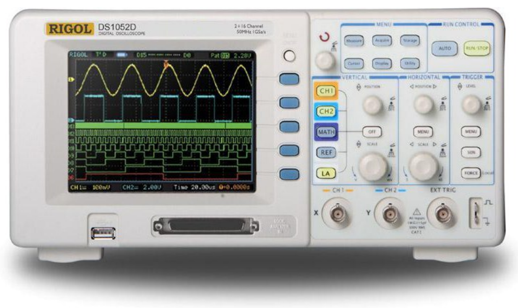

Figure 9: The oscilloscope [18]

A radioisotope gamma source (see Figure 10), used to artificially inflate the SiPM's detection rate, needed since the lab was located at ground floor in a large concrete building, where natural muon detection rates were too low for the fast-paced troubleshooting process. A breadboard and a power source was also used for testing the Op-Amps.

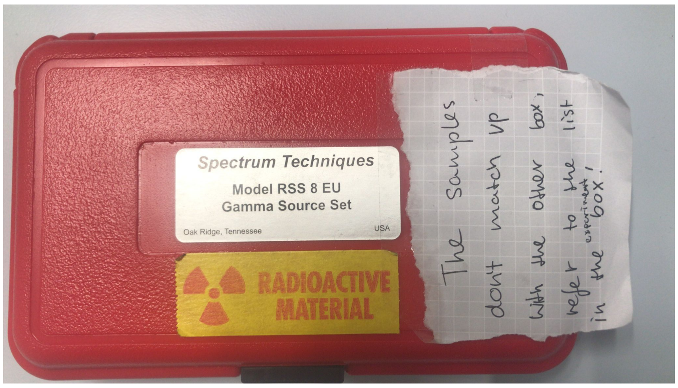

Figure 10: Radioisotope gamma source

3.4.2 Packaged Components Quality Check

The first (preliminary) phase of testing determined whether the unmounted simple components still in their packaging were labelled correctly and up to specs. This was done to avoid potentially replacing a broken component with another. Capacitors and resistors were confirmed to be within the error range presented on their packaging, if not within these bounds they would be labelled faulty. Ferrite beads were identified by use of a magnet.

3.4.3 Surface Mounted Capacitors and Resistors

The capacitors and resistors surface-mounted on the PCBs were visible and measurable using multimeters. This phase of testing was limited to only capacitors and resistors as they were the only components that could be easily tested while surface mounted. Three main PCBs were fully populated, together with three SiPM PCBs. Three SD card PCBs were missing the 3.3V voltage regulator component. Unfunctional PCBs were put aside and not included in further phases of testing.

3.4.4 Arduino Nano

The Arduino nanos mounted onto the main PCBs were readily testable. A micro-USB connection allows for code uploads which programs the Arduino. Uploading an empty code file works as a quick test to see if the Arduino is capable of resetting itself and receiving information from the USB connection. This test ruled out one of the three populated main PCBs, on which the Arduino was unresponsive, leaving us with two viable main boards.

3.4.5 Troubleshooting Guide

A troubleshooting guide on the github repository [10] outlines the steps necessary to determine where the fault lies in a broken detector. After having assessed the conditions of the individual PCBs in the previous phases of testing and collecting the most viable boards into one detector assembly, the troubleshooting guide, which only handled fully assembled and populated detectors, fell into scope and could be used to further identify problems.

Following the guide, the DC-DC boosters on the two main PCBs were measured by four of six female pin connectors which connect the main PCBs to the SiPMs. Two pairs of relevant pins are present, one pair for a positive voltage of 29.5V and one pair for ground. Measuring across these revealed the DC-DC boosters to be working normally, supplying a consistent voltage of 29.5V to the SiPMs.

Three test points are included on the main PCB. Each test point corresponds to one section of the circuitry. Measuring across them and ground using an oscilloscope to visualise the signal should reveal what sections of the main PCB are causing the detector to not be adding counts. Test point 1 was showing the expected peak, representing the raw output from the SiPM, on both main PCBs. Test point 2 and 3 however, were not showing the expected readings. The test points' sections each processed the signal after each other, the dysfunctional component was therefore in test point 2's section. Having tested all the simple components, the fault must lie in a more complicated device, test point 2 only had one such device, the dual OP-Amp (which it also shares with test point 3).

3.4.6 Op-Amps

An attempt to test the Op-Amps was made by soldering lengths of wire onto one and setting up a feedback loop circuit on the breadboard, powered by the power source. The oscilloscope showed no feedback and the Op-amps were determined to be faulty. This component being broken corresponded with the behavior of the defective assembled detectors. Testing ended and new Op-Amps were ordered.

3.5 Muon Detector Assembly

Once all components were identified, tested, and reordered (if needed), all components required to build one complete muon detector were organized into boxes. This was done to facilitate the people soldering and to easily test again all components used. After all was set up, the components were mounted onto the PCBs using solder paste and the hot air gun. Firstly, all resistors were pasted onto the board and then all the capacitors after that. The order was established by following the list published on the Cosmic Watch's GitHub (Figure 18).

Once all the small components were pasted onto the board, the bigger components were then also mounted on the board. Finally as all items on the list were mounted on the respective boards, all the PCBs were connected to each other using the respective headers and connectors. Finally, the code was uploaded to the arduino. To do so, the arduino IDE had to be downloaded from `https://www.arduino.cc/en/software`. Then the code had been copied from the cosmic watch website (`http://www.cosmicwatch.lns.mit.edu/`) and uploaded to the arduino. After the whole components list was exhausted and the code uploaded, the completed muon detector was tested using the test points on the main PCB. Due to time and equipment constraints only one whole muon detector was built from scratch, while another was completed with available components.

4 Results

4.1 Results obtained in this project

In this project, only one detector was built since there were some missing components; like already mentioned above. However, even this detector did not work either. This was very probably due to the op-amp that was broken. Indeed, the op-amp is one of the most sensitive components on the board. Moreover, because it was not possible to order some new op-amp online, the one of the previous group had been desoldered from their board and re-used. All these manipulations probably damaged this fragile component, resulting in some dysfunction in the final detector.

Nevertheless, it seemed that the SiPM worked properly: When the oscilloscope was connected to the SiPM, a peak was indeed detected as shown in Figure 11. This confirmed that the SiPM functioned as it should, generating a peak in the same form as could be expected from the instruction manual. It however did have a lower amplitude, suggesting a fault somewhere else.

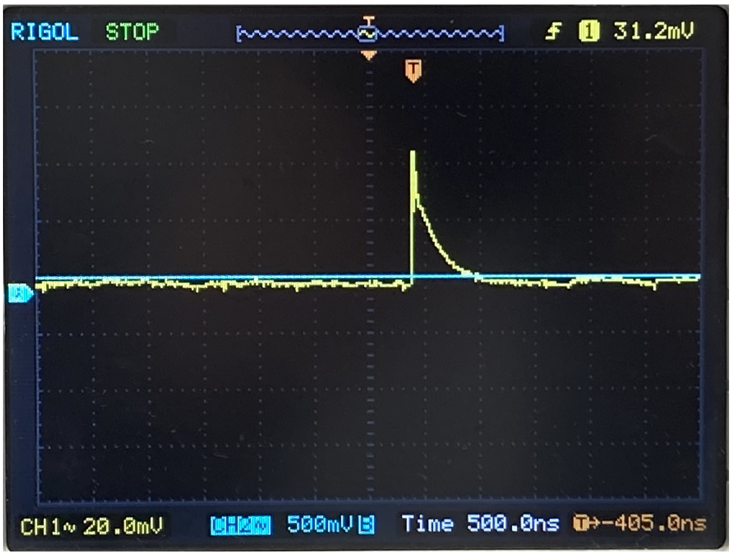

Figure 11: Peak from the SiPM detected by the oscilloscope

When connecting the oscilloscope to the amplification and to the peak detector (TP2 and TP3; see the circuit in Figure 2), no signal was detected. This indeed suggests that the op-amp was not working like it was supposed to. The following image illustrate what was the desired signal that should be measured if the PCB was working:

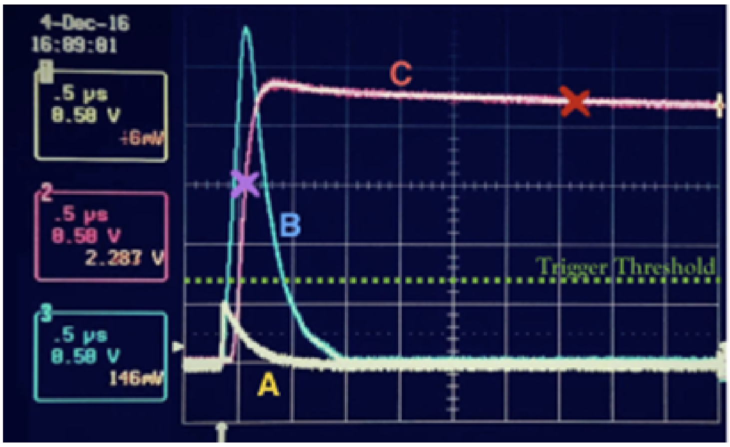

Figure 12: The 3 different signals supposed to get if the PCB was working correctly [10]

On this figure, A is the raw signal from the SiPM PCB; B is the signal after it went through the amplification circuit and C is what the signal looks like after the peak detector circuit (if needed use the Figure 2 for a better visualization) [10].

For the detector that was build in this project, only the signal A was visible (since the SiPM works correctly). However, the signal B and C were more problematic which is due to the op-amp not working properly like already mentioned earlier.

4.2 Expected Results

Because no concrete results were gathered during this project, this paragraph will instead explain what was expected. The ultimate objective was to build 5 detectors to combine the data of each detector to get a more accurate measurement and reduce error. This would allow us to look at the variation of muon detection depending on different parameters. The most interesting one is the influence of the altitude: The rate of detection is supposed to increase exponentially when the altitude is increasing, like the graphs below are showing (Figures 13 and 14) [10]. The Y axis represent the variation of the rate while the X axis the altitude:

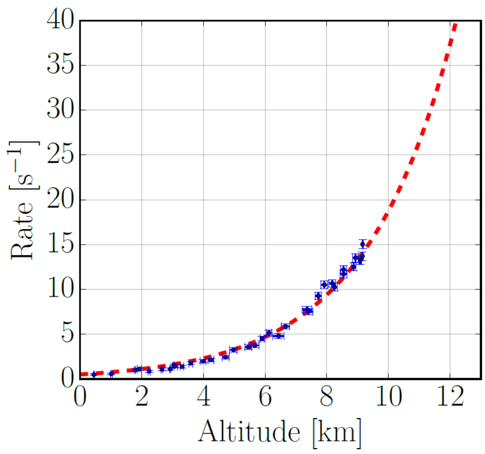

Figure 13: Variation of the muon detection rate depending on the altitude [10]

Additionally to the Figure 13, another interesting graph is shown in the Figure 14. This graph indeed represents how the rate is varying depending on altitude as well. More exactly it is showing the muon detection along a plane flight [10]: The X axis is the flight time and the Y axis the detection rate.

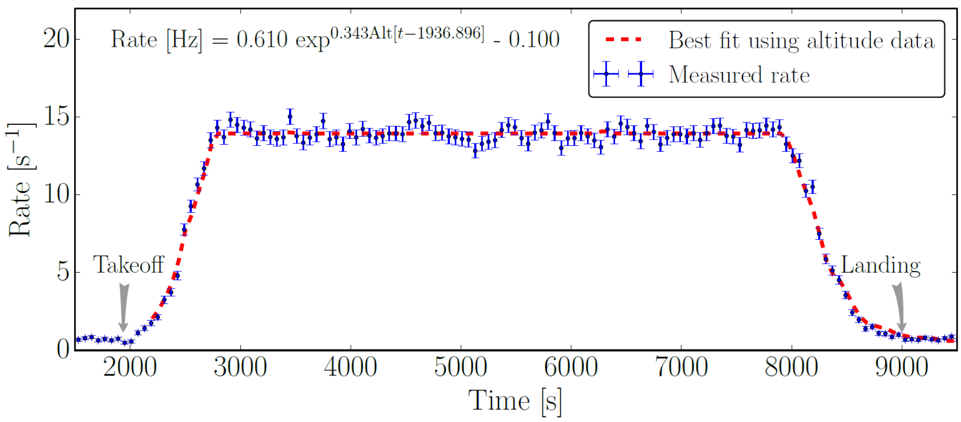

Figure 14: Muon detection along a plane flight [10]

Although the altitude seems to be the major factor that influences the detection rate, some other experiments can be performed as well. For instance, how the surroundings of the detector affect the rate (e.g., if the detector is inside a building vs if it is not). The detector built in this project would not have been capable of more precise measurement which will be discussed later in the paper. However, the idea of this project was a proof of concept for these detectors, and while this attempt wasn't successful, it will undoubtedly be showcased by future project groups at MSP.

5 Discussion

5.1 Component Troubles

As the construction of a Muon Detector had already been attempted by a previous group it was possible to continue work where the other group had to seize their progress. The previous group got quite far with the construction of their Muon detector but ultimately was unable to get it to work. This meant that the first days of the project required extensive troubleshooting of every component already mounted on the PCB. Along with testing every component, an inventory had to also be made to order components not present, replace broken components and restock up to a level where an attempt could be made at building 5 complete Muon Detectors. This whole organization process took up a whole week; in the meantime soldering and the hot air gun were being practiced on practice boards.

One of the biggest setbacks faced was the fact that the Op-Amps were not functioning, after the oscilloscope was replaced a signal roughly resembling what was to be expected was able to be observed but at a much lower amplitude, in fact low enough to often not trigger the threshold for detection. This alluded to the fact the Op-Amps were not working correctly. The op amp (LT1807) was suspected to be the problem, as a signal was detected from the SiPM and it could be seen when connecting the board to an oscilloscope through TP1(where the signal only goes through the SiPM and a 1k resistor); but once the oscilloscope was connected to TP2(where the peak detected should be amplified by the op amp) only noise was seen with some occasional peaks. Multiple tests were performed on the mounted Op-Amps by testing the inverting and non-inverting output (Figure 15).

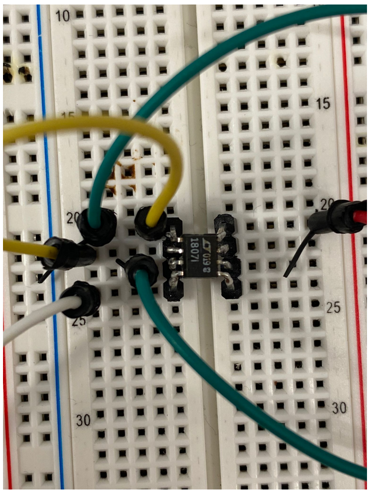

Figure 15: Op-Amp LT1807 being tested at its inverting and non-inverting inputs using a multimeter (out of frame)

Said tests were not successful, thus confirming that the Op-Amps were not working. This consequently meant the Muon detector could ultimately not be finished as new Op-Amps were not able to be acquired in time due to a global shortage at this moment. This then meant that the only possible way to effectively use the Muon detector would have been to have an oscilloscope constantly connected to TP1, with a camera capturing the oscilloscope screen. The footage would then have to be checked to count the peaks that appeared; this method was deemed unreasonable due to its time requirements and inaccuracy.

5.2 Scintillator

When the scintillator was wrapped in electrical tape, after having been wrapped in tin foil, various types of electrical tape were used - one black and two green ones. As it was clearly seen by testing the signal when the oscilloscope was connected to TP1, the black electrical tape worked better than others at reducing noise by making the scintillator light-proof most likely due to its color. To reduce the noise in the signal detected, the noisier scintillators were further wrapped with additional layers of electrical tape and some even with another layer of tin foil. Due to the abundance of scintillators taped to their respective PCBs, the least noisy ones were used for circuit troubleshooting and testing. The types of electrical tape can be seen in Figure 16.

(a) Black tape[19] (b) Yellow and green tape [20] (c) Green tape [21]

Figure 16: Types of electrical tapes

5.3 Delays

Due to having to wait for a full week on components it was only possible to start on Friday of the second week with attempting to build a Muon Detector from scratch as components had to arrive first. Further delay was caused when, late in the project, it was found out that the oscilloscope present in the lab was not working as it should. This undetected malfunction significantly set back the troubleshooting efforts during the latter stages of the project once a complete detector had been assembled. The faulty oscilloscope was then replaced with a working one.

The process of soldering was a lot slower than desirable, this due to the fact that there were only two actual soldering stations present, a heat gun with soldering paste and an actual soldering station. There was a tertiary station present in the lab but this station was unusable due to the soldering tip being too thick for the SMD soldering that was required during the project.

5.4 Applications of Muon Detectors

5.4.1 Muography

With the rise of accessible and affordable muon detectors, there has been growing applications for these tools which has prompted a so called ‘muon boom’. One of the main advantages of muons is how little they interact with matter, unlike X-rays, muons can easily pass through lead and other heavy atomic materials and measured on the otherside. This method, named muography or muon topography, offers a better way to peer into large or dense structures and map their inisdes. Contrary to X-ray or ultrasonic mapping, muons are naturally produced in homogeneous ways all around the Earth’s surface, which eliminates the need for a an emitter and drastically reduces costs while also increasing overall usability [22].

5.4.2 Archeological and Geological Applications

In 2017 a group of researchers used muography to scan the insides of one of the Great Pyramids of Giza, see Figure 17. By measuring the density and the rate of muons passing through a standard volume inside the pyramid, they can map out the space between detector and the sky. A larger rate of muons than the expected average in a specific direction would imply an empty space in the pyramid, which is how the group discovered a new chamber; a first since the 19th century. According to the researchers, three different muon detecting technologies were used: nuclear emulsion films, scintillator hodoscopes and gas detectors, all confirming the new void [23].

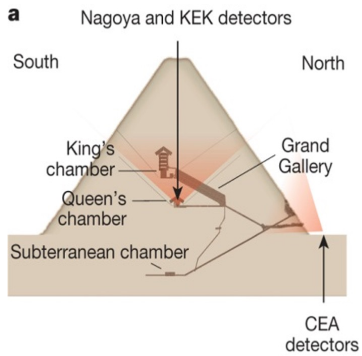

Figure 17: Diagram of the muography experiment performed in The Great Pyramid. The detector is in the Queen's chamber and the flux of muons is coming from above and through the stone. Another detector was placed outside to increase confidence in the measurements.

Similarly, this technique can be applied to the study of volcanoes which will help map out the internal dynamics of the volcanic structure. Such en experiment was conducted at the Stromboli volcano and reports new information on the eruptive dynamics and how they are controlled [24].

6 Conclusion

Looking back, this year's project seemed a good continuation of last year's even though no functioning detector was built. The mistakes that were made this time around allow for more precise advice and understanding for future attempts, such as where the circuits could have malfunctioning components. In the first week of this project, an inventory of the components left from the last project's attempt was made, then any missing items were ordered at the start of the second week. During this second week, troubleshooting of the old boards aimed to find what went wrong and some people trained at soldering on practice boards. The components ordered arrived at lunch on the Friday of week 2, and the PCBs were finished on the Monday of week 3. The defect in the oscilloscope was found out on the next day, and the Op-Amps were labeled as faulty on the Wednesday of the same week. New Op-Amps were ordered right after finding this out, but as they could not arrive on time, construction of a working detector was ruled out. Further work was limited due to the writing of this report and making the presentation.

For future reference, to be able to finish the project on time and hope to use the detectors, it is advised to order all the components from scratch as soon as possible while following the components list (especially for the op-amp, DC/DC booster, the Arduino and SiPM photodiode, which are the most fragile components and are difficult to get). Possibly order a slight excess of the fragile components, such as the DC-DC booster, in case that if some break, spare ones are readily available. Recommended websites are Digikey or Mouser if the shipping delay is not too long. Otherwise, Farnell can provide faster shipping, but it does not have all the components. Lastly, tidying up and cleaning up the lab while still working in it will help stay organized.

7 Appendices

7.1 Contributions

Coolen Finn	Did Inventory of parts; desoldered some parts in week 1 and 2, helped with troubleshooting at the end of week 2 with testing the Op-Amps and SiPM and helped writing the results and parts of the discussion section.
Gévers Nicolas	General formatting and setup of the latex document, editing and adding to multiple sections. Experimenting with the different soldering methods and cleanup of the lab. Generated the 3D model of the detector, will be heavily involved in the animation and overall design of the presentation.
Hangelbroek Renée	Inventory of parts; looking for components online and find alternative components that were not available; theory; introduction; final edits on the report(grammar, spelling, consistency).
Louveau Nicolas	Inventory of part; helped for troubleshooting; finding all the components to order online (Farnell) and finding alternative components for the one that was not available; organizing the components to build the new board and desoldering from the old board the necessary components; helped to solder the new board from scratch; looked into troubleshooting with oscilloscope and uploading the code to Arduino; writing of the 'soldering' section (in method), of the 'ordering the missing component' section and of the result section; helped clearing out the lab and reorganizing components/parts/boards for future project teams.
Palmerio Jeremy	Inventory of parts; troubleshooting the SiPM and the PCBs; tested components on old PCBs to determine point of failure; re-flowed components on the board in hope of fixing them; built 2 functioning SiPMs; helped build a new board from scratch; tested op amps using breadboard and oscilloscope and attempted to order new op amps; contributed to writing the electronic description in the methods, materials, experimental uses in the discussion and some of the results.
Ranaudo Guglielmo	Inventory of parts; troubleshooting the SiPM and the PCBs; tested components on old PCBs to determine point of failure; re-flowed components on the board in hope of fixing them; prepared, tested and desoldered components used to build new board; helped build a new board from scratch; tested op amps using breadboard and oscilloscope and attempted to order new op amps; contributed to writing discussion, method for the assembly of a muon detector and overall corrections in the paper; helped clearing out the lab and reorganizing components/parts/boards for future project teams.
Roussel Edgar	Inventory of parts; Researched background theory and wrote the conclusion; helped correcting mistakes present over the paper; made 3D models of the detector in collaboration with Nicolas Gévers to allow for a better visualization; helped clearing out the the lab and reorganizing components/parts/boards for future project teams.
Verloo Matijs	Inventory of parts; troubleshooting the SiPM and the PCBs; tested components on old PCBs to determine point of failure; Tested Arduino Nanos; Sorted existing PCB boards based on level of functionality; contributed to writing method's testing part and conclusion.

7.2 Components reference list

PCB populating reference

Component	value	Discription	Link	Comment
R1	10k	RES SMD 10K OHM 1% 1/8W 0805	Digikey Part Number: 311-10.0KCRCT-ND	
R2	226k	RES SMD 226K OHM 1% 1/8W 0805	Digikey Part Number: 311-226KCRCT-ND	
R3	249	RES SMD 249 OHM 1% 1/4W 0805	Digikey Part Number: 311-249CRCT-ND	
R4	1k	RES SMD 1K OHM 1% 1/8W 0805	Digikey Part Number: 311-1.00KCRCT-ND	
R5	10k	RES SMD 10K OHM 1% 1/8W 0805	Digikey Part Number: 311-10.0KCRCT-ND	
R6	100k	RES SMD 100K OHM 1% 1/8W 0805	Digikey Part Number: 311-100KCRCT-ND	
R7	100k	RES SMD 100K OHM 1% 1/8W 0805	Digikey Part Number: 311-100KCRCT-ND	
R8	1k	RES SMD 1K OHM 1% 1/8W 0805	Digikey Part Number: 311-1.00KCRCT-ND	
R9	Short	RES SMD 0 OHM JUMPER 1/8W 0805	Digikey Part Number: 311-0.0ARCT-ND	SHORT
R10	NS			
R11	49.9	RES SMD 49.9 OHM 1% 1/8W 0805	Digikey Part Number: 311-49.9CRCT-ND	
R12	49.9	RES SMD 49.9 OHM 1% 1/8W 0805	Digikey Part Number: 311-49.9CRCT-ND	
R13	49.9	RES SMD 49.9 OHM 1% 1/8W 0805	Digikey Part Number: 311-49.9CRCT-ND	
R14	NS			
R15	1k	RES SMD 1K OHM 1% 1/8W 0805	Digikey Part Number: 311-1.00KCRCT-ND	
R16	10k	RES SMD 10K OHM 1% 1/8W 0805	Digikey Part Number: 311-10.0KCRCT-ND	
R17	Short	RES SMD 0 OHM JUMPER 1/8W 0805	Digikey Part Number: 311-0.0ARCT-ND	Short
R18	NS			
R19	NS			NS
R20	10k	RES SMD 10K OHM 1% 1/8W 0805	Digikey Part Number: 311-10.0KCRCT-ND	
R24	24.9k	RES SMD 24.9K OHM 1% 1/8W 0805	Digikey Part Number: RMCF0805FT24K9CT-ND	
R25	NS			NS
D1	500ma diode	DIODE SCHOTTKY 40V 500MA SOD123	Digikey Part Number: MBR0540CT-ND	**Has direction**
D2	500ma diode	DIODE SCHOTTKY 40V 500MA SOD123	Digikey Part Number: MBR0540CT-ND	**Has direction**
L1	47uH	FIXED IND 47UH 170MA 1.3 OHM SMD	Digikey Part Number: 490-4063-1-ND	
L2	2.5k Ferrite Bead	FERRITE BEAD 2.5 KOHM 0805 1LN	Digikey Part Number: 587-1919-1-ND	
C1	22pF	CAP CER 22PF 50V NP0 0805	Digikey Part Number: 399-1113-1-ND	
C2	0.47uF	CAP CER 0.47UF 50V X7R 0805	Digikey Part Number: 399-8100-1-ND	
C3	1uF	CAP CER 1UF 50V Y5V 0805	Digikey Part Number: 587-1308-1-ND	
C4	10uF	CAP CER 10UF 6.3V X5R 0805	Digikey Part Number: 490-1718-1-ND	
C5	0.1uF	CAP CER 0.1UF 50V X7R 0805	Digikey Part Number: 399-1170-1-ND	
C6	20nF	CAP CER 20nF 50V X7R 0805	Digikey Part Number: 1276-2472-1-ND	
C7	10.0pF	CAP CER 10PF 50V C0G/NP0 0805	Digikey Part Number: 1276-1109-1-ND	
C8	10 nF	CAP CER 10000PF 50V X7R 0805	Digikey Part Number: 311-1136-1-ND	
C9	10 nF	CAP CER 10000PF 50V X7R 0806	Digikey Part Number: 311-1136-1-ND	
C10	10 nF	CAP CER 10000PF 50V X7R 0807	Digikey Part Number: 311-1136-1-ND	
C11	10 nF	CAP CER 10000PF 50V X7R 0808	Digikey Part Number: 311-1136-1-ND	
C14	Short	RES SMD 0 OHM JUMPER 1/8W 0805	Digikey Part Number: 311-0.0ARCT-ND	SHORT
C15	0.1uF	CAP CER 0.1UF 50V X7R 0805	Digikey Part Number: 399-1170-1-ND	
C16	10uF	CAP CER 10UF 6.3V X5R 0805	Digikey Part Number: 490-1718-1-ND	
C17	0.1uF	CAP CER 0.1UF 50V X7R 0805	Digikey Part Number: 399-1170-1-ND	
C18	1uF	CAP CER 1UF 50V Y5V 0805	Digikey Part Number: 587-1308-1-ND	
U1	LT3461	3MHz Step-Up DC/DC Converters	http://www.linear.com/product/LT3461A	Has direction
U2	LT1807IS8#PBF	325MHz, Dual, Rail-to-Rail Input and Output, Precision Op Amps	http://www.linear.com/product/LT1807	Has direction
U7	NS			NS
U6	3.3V regulator	IC REG LINEAR 3.3V 300MA SOT23-3	Digikey part number: AP2210N-3.3TRG1DICT-ND	Has direction
U8	SD card socket	SMT SMD Cell Phone TF Micro SD Memory Card Slot Holder Sockets	Amazon: uxcell 6 Pcs SMT SMD	
U10	Non-Inverting Buffer	High Speed CMOS Logic Hex Non-Inverting Buffers	Mouser Part Number: 595-CD74HC4050M96,	Has direction
SiPM1	SiPM	SiPM MicroFC-60035-SMT	SENSL	Has direction
Reset	Reset button	SWITCH TACTILE SPST-NO 0.02A 15V	Digikey part number: P12215S-ND	
2x4 SD header	2x3 header +2x1	header for mounting SD card PCB. 2x3 + 1x2	Comes with Arduino	
15x1 header	15x1 header	2x headers for mounting Arduino, should come with Arduino	Comes with Arduino	
Arduino_Nano	Arduino Nano	16 MHz CH340/ATmega328P Arduino Nano		
BNC receptacle	BNC header	CONN BNC JACK R/A 50 OHM PCB	Digikey part number: WM5514-ND	
OLED header	4 pin header	CONN FEMALE 4POS .100" R/A TIN	Digikey part number: S5440-ND	Bottom
LED	LED light	Any color, 5mm	https://www.amazon.com	
6-pin Header	6-pin Header	SOCKET 7 MM SOLDER TAIL DOUBLE	Digikey Part Number: 1212-1229-ND	
3.5 mm jack	3.5mm jack	CONN JACK 4COND 3.5MM SMD R/A	Digikey Part Number: CP-43515RSSJCT-ND	
Temp	TMP36	Temperature Sensors TMP36 Precision Linear Analog Output		
SiPM PCB 6-Pin	6-pin Pins	WM17457-ND	WM17457-ND	

Main PCB
SiPM PCB
SD card PCB

Figure 18: Components reference list[25]

References

[1] CERN. *Cosmic Rays discovered 100 years ago*. Aug. 2012. URL: https://home.cern/news/news/physics/cosmic-rays-discovered-100-years-ago.

[2] Spencer Axani et al. *CosmicWatch*. Web Page. URL: http://www.cosmicwatch.lns.mit.edu/.

[3] Pierre Auger Observatory. *The Mystery of High-Energy Cosmic Rays*. Electronic Article. URL: https://www.auger.org/outreach/cosmic-rays/cosmic-ray-mystery.

[4] S.C. Griffin. *THE EAST-WEST COSMIC MUON ASYMMETRY*. Pamphlet. URL: http://www.physics.mcgill.ca/~griffins/muon_poster.pdf.

[5] Pham Ngoc Dinh et al. "Measurement of the vertical cosmic muon flux in a region of large rigidity cutoff". In: *Nuclear Physics B* 627.1 (2002), pp. 29–42. ISSN: 0550-3213. DOI: https://doi.org/10.1016/S0550-3213(02)00063-9. URL: https://www.sciencedirect.com/science/article/pii/S0550321302000639.

[6] P.K.F. Grieder. *Cosmic Rays at Earth, Researcher's Book Manual and Data Book*. Electronic Book. 2001. URL: http://theor.jinr.ru/~vnaumov/Eng/JINR_Lectures/books/Grieder2001.pdf.

[7] Physics4students. *Latitude Effect of Cosmic Rays*. Film or Broadcast. Jan. 2017. URL: https://www.youtube.com/watch?v=LQBTsTRY2Rw.

[8] G. Lemaitre Vallarta and M. S. "On Compton's Latitude Effect of Cosmic Radiation". In: *American Physical Society* 43.2 (1933). DOI: https://doi.org/10.1103/PhysRev.43.87.

[9] Zhenzhou Deng and Anyi Li. *A Novel Visible Light Communication System Prototype Based on SiPM Receiver*. 2019. DOI: 10.48550/ARXIV.1909.00641. URL: https://arxiv.org/abs/1909.00641.

[10] spenceraxani. *CosmicWatch-Desktop-Muon-Detector-v2/Instructions.pdf*. 2018. URL: https://github.com/spenceraxani/CosmicWatch-Desktop-Muon-Detector-v2/blob/master/Instructions.pdf.

[11] Zhenzhou Deng and Anyi Li. *A Novel Visible Light Communication System Prototype Based on SiPM Receiver*. 2019. DOI: 10.48550/ARXIV.1909.00641. URL: https://arxiv.org/abs/1909.00641.

[12] Marc de Vinck. *Getting started with soldering*. en. Sebastopol, CA: Maker Media, Oct. 2017.

[13] Charles R. Hampton. *Tools and techniques for hot air soldering surface-mount components - projects*. Apr. 2017. URL: https://www.allaboutcircuits.com/projects/tools-techniques-hot-air-soldering-surface-mount-components/.

[14] Collin Cunningham. *Collin's lab: Soldering*. June 2014. URL: https://learn.adafruit.com/collins-lab-soldering.

[15] *A 500g reel of 22swg 60/40 Solder*. URL: https://upload.wikimedia.org/wikipedia/commons/thumb/3/3d/60-40_Solder.jpg/616px-60-40_Solder.jpg?20060916014901.

[16] *Datasheet Stock No. 124-4134*. URL: https://docs.rs-online.com/79ca/0900766b81560388.pdf.

[17] *VOLTCRAFT SMD-200 Multimeter Digitaal CAT III 600 V*. e-store website. URL: https://www.amazon.nl/dp/B003A61GOU/ref=asc_df_B003A61GOU1654259400000/?creative=380333&creativeASIN=B003A61GOU&linkCode=asn&tag=beslistnl20-21&ascsubtag=7261146f-4da7-4c4e-8f47-8fcb4ab15f74.

[18] *Rigol DS1052D oscilloscoop*. e-store website. URL: https://www.eleshop.nl/rigol-ds1052d-oscilloscoop.html.

[19] BOLTS N' MORE. Figure. 2022. URL: https://www.boltsnmore.com/product/electrical-tape/.

[20] CABLEMATIC. Figure. 2022. URL: https://cablematic.com/en/products/015x19mm-yellow-green-electrical-tape-in-20m-coil-BS098/.

[21] PacRad. Figure. 2022. URL: https://www.pacrad.com/3m-35-1-2-5.html.

[22] David Adam. "Muography offers a new way to see inside a multitude of objects". In: *Proceedings of the National Academy of Sciences* 118.14 (2021), e2104652118. DOI: 10.1073/pnas.2104652118. eprint: https://www.pnas.org/doi/pdf/10.1073/pnas.2104652118. URL: https://www.pnas.org/doi/abs/10.1073/pnas.2104652118.

[23] Kunihiro Morishima et al. "Discovery of a big void in Khufu's Pyramid by observation of cosmic-ray muons". In: *Nature* 552.7685 (Dec. 2017), pp. 386–390. ISSN: 1476-4687. DOI: 10.1038/nature24647. URL: https://doi.org/10.1038/nature24647.

[24] Valeri Tioukov et al. "First muography of Stromboli volcano". In: *Scientific Reports* 9.1 (Apr. 2019), p. 6695. ISSN: 2045-2322. DOI: 10.1038/s41598-019-43131-8. URL: https://doi.org/10.1038/s41598-019-43131-8.

[25] spenceraxani. *CosmicWatch-Desktop-Muon-Detector-v2/blob/master/$PCB_Files/SMT_reference.pdf$*. 2018. URL: https://github.com/spenceraxani/CosmicWatch-Desktop-Muon-Detector-v2/blob/master/Instructions.pdf.